Plant Cell Tiss Organ Cult (2015) 122:453–463
DOI 10.1007/s11240-015-0782-7

ORIGINAL PAPER

Metabolomics reveals distinct methylation reaction in MeJA elicited *Nigella sativa* callus via UPLC–MS and chemometrics

Mohamed A. Farag[1] · Abeer M. El Sayed[1] · Ahmed El Banna[1] · Susanne Ruehmann[2]

Received: 5 February 2015 / Accepted: 3 May 2015 / Published online: 13 May 2015
© Springer Science+Business Media Dordrecht 2015

Abstract Cell suspension cultures are now recognized as important model for studying natural products biosynthesis and functional genomics. Nevertheless, very few studies of metabolic comparisons between cell cultures (callus) and original plants have been reported, even though the biological identity of cultured cells with the normally grown plant is of great importance. In this study, an MS-based metabolomic approach was used to compare the natural products profile of intact *Nigella sativa* seeds versus callus. *N. sativa* has been used for centuries in traditional medicine for several purposes. Its phytochemical components comprise, among others, alkaloids, saponins, flavonoids and fatty acids. Ultra performance liquid chromatography coupled to ultraviolet photodiode array detection and high resolution q-TOF mass spectrometry (UPLC–PDA–MS) was utilized to analyze the secondary product metabolome of *N. sativa* callus, with a total of 74 metabolites including five flavonoids, 13 hydroxycinnamates, an alkaloid, saponin and 14 fatty acids. Callus maintained the capacity to produce *N. sativa* phenolic subclasses, with hydroxycinnamates amounting for the major secondary metabolites in callus. Alkaloids, major constituents in *Nigella* genus, were detected in callus though with qualitative and quantitative differences from seed tissue. Methyl jasmonate (MeJA) elicitation effect was assessed on callus with the aim of increasing secondary metabolites production. Metabolite profiles were subjected to principal component analysis and orthogonal projection to latent structures-discriminant analysis to evaluate MeJA effect. Results revealed that MeJA led to *O*-methylation reaction induction yielding *O*-feruloylquinic acid from *O*-caffeoylquinic acid, in addition to a methylated disaccharide. The work extends our knowledge regarding hydroxycinnamates biosynthesis, regulation and on metabolic engineering future efforts to increase its production as potential phytoalexin in *N. sativa*.

Keywords *Nigella sativa* · Metabolomics · Cell culture · *O*-feruloylquinic acid · Methyl jasmonate · UPLC–MS · Phytoalexins

Introduction

Nigella sativa L. (black cumin), commonly known as black seed, is a member of the Ranunculaceae family native to Southwest of Asia. *N. sativa* seed has been regarded as a blessing and healing food additive in Middle Eastern culture (Moghaddasi 2011) used as an important nutritional favoring agent, traditional folk and natural health remedy for the treatment of numerous ailments (Randhawa and Alghamdi 2011). The seeds of *N. sativa* contain a myriad of constituents including fixed and essential oils, proteins, alkaloids, flavonoids and saponins (Liu et al. 2011; Khan 1999). These constituents mediate for *Nigella* well reported biological effects including antimicrobial (Rafati et al. 2014), anti-inflammatory and antioxidant activities, asthma treatment, and in chemoprevention (Sultan et al. 2014; Ahmed et al. 2013; Al-Kalaf and Ramadan 2013). Phenolics such as di-thymoquinone, thymoquinone, thymol, and carvacrol enriched in black cumin are of increasing interest

✉ Mohamed A. Farag
mfarag73@yahoo.com; Mohamed.farag@pharma.cu.edu.eg

[1] Pharmacognosy Department, Faculty of Pharmacy, Cairo University, Kasr El-Einy Street, Cairo 11562, Egypt

[2] TUM School of Life Sciences Weihenstephan, Technische Universität München, Gewächshauslaborzentrum Dürnast, 85354 Freising, Germany

due to its well characterized biological effects including analgesic (Houghton et al. 1995), antioxidant (Burits and Bucar 2000), anti-inflammatory (Xuan et al. 2010) and anticancer properties (Kumara and Huat 2001). Antiviral effect of black seed oil was analyzed using murine cytomegalovirus (Salem and Hossain 2000). Recently, anti-inflammatory and cytotoxic effect of *N. sativa* seeds and its callus extract was investigated in context to its thymoquinone content (Al-Sheddi et al. 2014; Alemi et al. 2013).

Modern plant biotechnology approaches i.e., plant cell and tissue culture provide scientists with alternatives for the production of bioactive natural products, there is increasing interest in studying the biochemical properties of proliferated plant cells under artificial conditions and comparing it with that of differentiated native plants. Callus induction of black cumin was previously reported, albeit without metabolites characterization (Banerjee and Gupta 1975). Cytological abnormalities in callus cells during sub-cultures and with changes in its thymol content (Chand and Roy 1979; Al-Ani 2008) were also observed.

As is the case in most plant defense response, it is very unlikely that one but rather several compounds are involved in plant resistance, the identity of which are, a priori, unknown (Leiss et al. 2009). Phytoalexins are natural products produced by plants in response to microbial infection, varying from acetylenic compounds, terpenoids, steroids, alkaloids to polyphenols especially isoflavonoids (Timperio et al. 2012). In some natural host/pathogen systems, phytoalexin production is initiated in response to certain specific elicitors i.e., methyl jasmonate (MeJA), methyl salicylate, chitin or yeast extract (Cui et al. 2013; Farag et al. 2009). Phytoalexin accumulation in plant cells usually occur within 6–24 h post elicitation suggesting that they are *denovo* synthesized in response to upstream defense genes up regulation (Guo et al. 1998). An example of phytoalexins occurrence in *planta* include caffeoylquinic acids derived from the phenylpropanoid pathway, known to be involved in plant biotic and abiotic stress responses. Caffeoylquinic acids (mono- and di-esters) were found at high levels in newly formed organs confirming their protective role in *Coffea canephora* leaf (Mondolot et al. 2006).

Only few reports describe the analysis of phytoalexins production in *N. sativa* callus. Although *N. sativa* is itself a very competitive target for phytochemical studies, nothing is known on the comparative chemical composition of *N. sativa* and its undifferentiated cell using large scale untargeted analytical techniques and in response to chemical elicitations. The technology of metabolomics is concerned with the comprehensive analysis of metabolites as a whole in a given sample. It has been successfully applied to characterize, identify and quantify metabolites in plant materials, increasingly against the background of intraspecific variability. Metabolomics or metabolites profiling became only possible with the recent advance in molecule separation and identification technologies, as well as novel programs that can rapidly process spectral or chromatographic patterns (Sumner et al. 2014). Such an approach has been used for elucidating isoflavonoids (phytoalexins) formation in the model legume *Medicago truncatula* (2009) as part of a functional genomics project, leading to the discovery of several new compounds, novel pathways and providing tools for efficient metabolic engineering of these bioactive chemicals.

The goal of this study was to obtain a more holistic metabolomic data set of *Nigella sativa* undifferentiated cells in comparison to its seeds (official organ used in Pharmacoepeas) and to further monitor cellular metabolites reprogramming in response to elicitation with the wound signal methyl jasmonate (MeJA, an insect herbivore mimic). Previous studies using targeted metabolites profiling have demonstrated that MeJA elicits the accumulation of several phytoalexin classes (Demkura et al. 2010). The adopted metabolomics approach in this study focused on chromatographic hyphenated ultra performance liquid chromatography UPLC/(−)ESI–qTOF–MS which has been previously applied for quality control analysis of *Nigella* seeds (Farag et al. 2014). The plant metabolomics using UPLC–qTOF–MS is relatively new and has been increasingly utilized in the field of plant metabolomics (Grata et al. 2008). UPLC coupled with qTOF–MS, can also detect chemical compounds with high sensitivity (Farag et al. 2013). Owing to the complexity of acquired data, multivariate data analysis i.e., principal component analysis (PCA) and orthogonal projection to latent structures-discriminant analysis (OPLS-DA) were also performed to define both similarities and differences among samples.

Materials and methods

Plant material

Nigella sativa seeds were provided by Dr. Andreas Heiss (University of Wien, Austria) and were used for production of callus.

Chemicals and reagents

Acetonitrile and formic acid (LC–MS grade) were obtained from J. T. Baker (The Netherlands), milliQ water was used for UPLC analysis. Standard for thymoquinone, chlorogenic acid, hederagenin, and kaempferol were purchased from Chromadex (USA). Chromoband C18 (500 mg, 3 ml) cartridge was purchased from Macherey and Nagel (Düren, Germany). All other chemicals and standards were provided by Sigma Aldrich (St. Louis, MO, USA). MeJA was provided by Bedoukian (USA).

Callus production and elicitation

Callus cultures were initiated from root and sprout segments of 3 weeks old *N. sativa* seedlings grown on filter paper bridges in glass tubes (15 × 150 mm) containing 10 ml a modified MS medium (Murashige and Skoog) supplemented with 40 g/l sucrose, 0.2 mg/l benzyl aminopurine and 10 mg/l indole acetic acid. At 4-week intervals, the calli were divided and transferred to a new medium. For experimental purpose the callus was propagated for 14 days at 22 °C under 16 h light conditions (60 µE m^{-2} s^{-1}) before the elicitation was executed. The incubation conditions were maintained throughout the whole study. For MeJA elicitation, 100 µl of a 50 mM solution of MeJA prepared in water was added to culture flasks to achieve a final concentration of 500 µM (Farag et al. 2009).

Extraction procedure and sample preparation for UPLC–MS analyses

Freeze dried *Nigella* callus and seed tissue were cooled in liquid nitrogen and ground with a pestle in a mortar. The powder (22 mg) was then homogenized with 1.8 ml 100 % MeOH containing 10 µg/ml umbelliferone (as internal standard for relative quantification using UPLC/MS) using ultrasonic bath for 20 min. Extracts were then vortexed vigorously and centrifuged at 12,000*g* for 5 min to remove plant debris and filtered through 22 µm pore size filter. Three µl were used for analysis. For each specimen, three biological replicates were provided and extracted in parallel under identical conditions.

High resolution UPLC–PDA–MS analyses

High resolution mass was measured for metabolites after UPLC separation. Chromatographic separations were performed on an Acquity UPLC system (Waters) equipped with a HSS T3 column (100 × 1.0 mm, particle size 1.8 µm; Waters) applying the following binary gradient at a flow rate of 150 µl min^{-1}: 0–1 min, isocratic 95 % A (water/formic acid, 99.9/0.1 [v/v]), 5 %B (acetonitrile/formic acid, 99.9/0.1 [v/v]); 1–16 min, linear from 5 to 95 % B; 16–18 min, isocratic 95 % B; 18–20 min, isocratic 5 % B. The injection volume was 3.1 µl (fullloop injection). Eluted compounds were detected from *m/z* 100–1000 using a MicroTOF-Q hybrid quadrupole time-of-flight mass spectrometer (Bruker Daltonics) equipped with an ApolloII electrospray ion source and negative ion mode using the following instrument settings: nebulizer gas, nitrogen, 1.6 bar; dry gas, nitrogen, 6 l min^{-1}, 190 °C; capillary, −5500 V (+4000 V); end plate offset, −500 V; funnel 1 RF, 200 Vpp; funnel 2 RF, 200 Vpp; in-source CID energy, 0 V; hexapole RF, 100 Vpp; quadrupole ion energy, 5 eV; collision gas, argon; collision energy, 10 eV; collision RF 200/400 Vpp (timing 50/50); transfer time, 70 µs; prepulse storage, 5 µs; pulser frequency, 10 kHz; spectra rate,3 Hz. Internal mass calibration of each analysis was performed by infusion of 20 µl 10 mM lithium formiate in isopropanol/water, 1/1 (v/v), at a gradient time of 18 min using a diverter valve.

MS data processing for multivariate analysis (PCA) and (OPLS)

Relative quantification and comparison of *Nigella* sprout and root derived callus metabolic profiles after UPLC–MS were performed using XCMS data analysis software under R 2.9.2 environment, which can be downloaded for free as an R package from the Metlin Metabolite Database (http://137.131.20.83/download/) (Smith et al. 2006). This software approach employs peak alignment, matching and comparison, as described in (Farag and Wessjohann 2012) to produce a peak list. The resulting peak list was processed using the Microsoft Excel software (Microsoft, Redmond, WA), where the ion features were normalized to the total integrated area (1000) per sample and imported into the R 2.9.2 software package for PCA and orthogonal projection to OPLS-DA. Absolute peak area values were autoscaled (the mean area value of each feature throughout all samples was subtracted from each individual feature area and the result divided by the standard deviation) prior to PCA. This provides similar weights for all the variables. PCA was then performed on the MS-scaled data to visualize general clustering, trends, and outliers among the samples on the scores plot. Orthogonal projection to OPLS-DA was performed with the program SIMCA-P Version 13.0 (Umetrics, Umeå, Sweden). Biomarkers for organs were subsequently identified by analysing the S-plot, which was declared with covariance (p) and correlation (pcor). The PCA was run for obtaining a general overview of the variance of metabolites, and OPLS-DA was performed to obtain information on differences in the metabolite composition among samples. Distance to the model (DModX) test was used to verify the presence of outliers and to evaluate whether a submitted sample fell within the model applicability domain.

Results and discussion

Major metabolite differences between undifferentiated cells and seed via UPLC–PDA–MS

Callus induction was generated from *N. sativa* by taking samples from both root and sprout tissue derived from

3 weeks old seedling. Qualitative and quantitative comparative analyses of *N. sativa* callus and its seed methanol extract were performed to determine the impact of dedifferentiation and culturing on *N. sativa*. Chemical constituents of extracts were analyzed via UPLC/PDA/(−)ESI–qTOF–MS, using a gradient mobile phase consisting of acetonitrile and aqueous formic acid that allowed for a comprehensive elution of all analytes i.e. phenolic acids, flavonoids, alkaloids and fatty acids within 16 min (ca. 1000 s) following a method developed for *N. sativa* seeds analysis (Farag et al. 2014). The elution order of the phenolics followed a sequence of decreasing polarity, whereby phenolic acids eluted first followed by flavonoid di glucosides, mono glucosides, alkaloids, free aglycones and fatty acids. Simultaneously acquired UPLC–MS total ion chromatograms of *N. sativa* callus extracts along with its seeds in negative ionization mode are presented in Fig. 1. The identities, retention times, characteristic observed molecular and fragment ions for individual components are presented in Table 1. A total of 74 metabolites were detected, of which 34 were identified. It is worth noting that this is the first comprehensive metabolite profile of *N. sativa* callus constituting such a large number of compounds. Metabolite assignments were made by comparing retention time, UV/vis spectra and MS data (accurate mass, isotopic distribution and fragmentation pattern in negative ion mode) of the compounds detected with *Nigella* compounds reported in the literature (Farag et al. 2014) and databases. A detailed description of the *N. sativa* seeds peak identifications and strategy has been published elsewhere (Farag et al. 2014). In callus, identified metabolites belonged to various classes (Table 1) including phenolic acids (i.e. *p*-coumaroylquinic acid), alkaloids (i.e. norargemonine), flavonoids (i.e. quercetin), terpenes (i.e. nigellic acid) and fatty acids (i.e. hydroxy-9,11-octadecadienoic acid), with phenolic acids (hydroxycinnamates) followed by fatty acids as the most abundant classes in both root and sprout derived callus. Photodiode array detection provided an overview of the main polyphenol classes (Fig. 1). UV–Visible spectra (200–600 nm) were recorded for different flavonoid subclasses including flavans (5, 6), flavonols (25–27, 30, 32) and hydroxycinnamates (8–18). Each sub-class has a characteristic UV spectrum (Mabry et al. 1970). For example, hydroxycinnamates typically have a maximum absorbance near 280 nm with a second maximum around 325 nm (9), whereas flavonols have maximum around 340–355 nm (30).

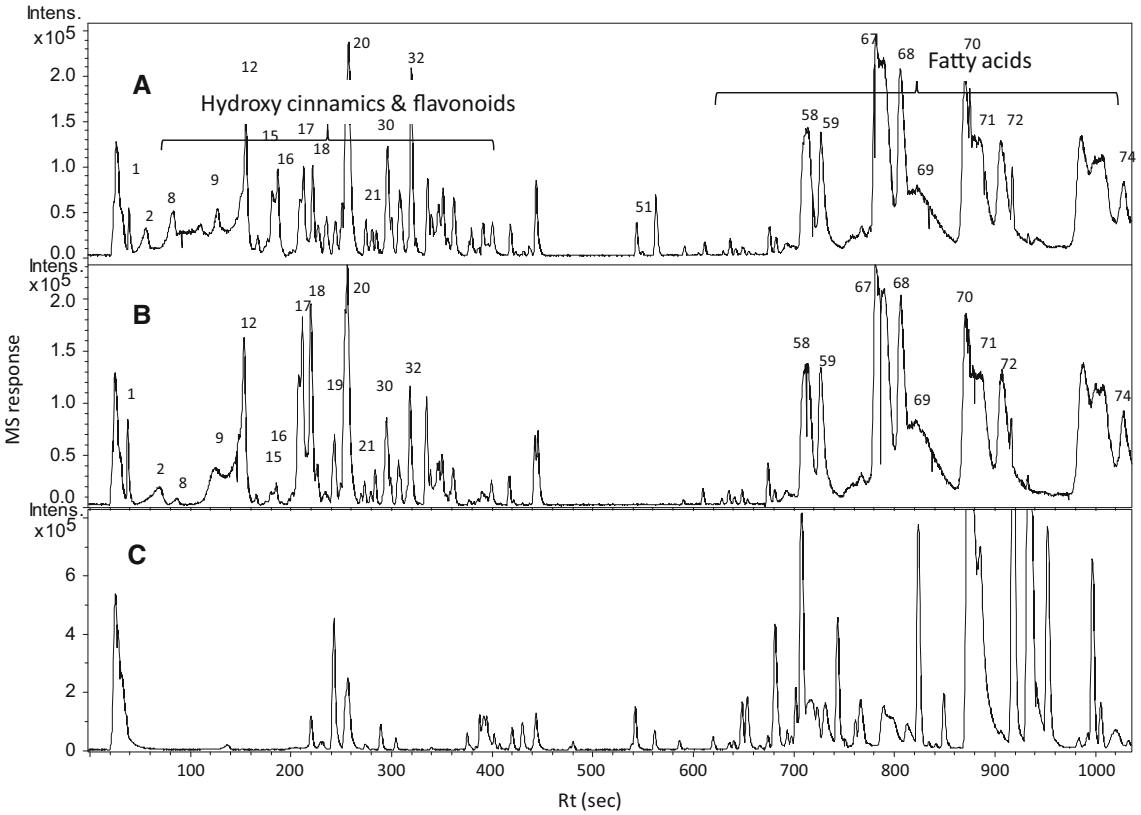

Fig. 1 UPLC–qTOF–MS base peak chromatograms of the methanol extracts of *Nigella sativa* callus derived from seedling sprout (**a**) and root (**b**) in comparison to that of seed (**c**) analysed under same conditions. Chromatographic conditions are described under "Materials and methods". The identities, R_t-values, and basic UV and MS data of all *peaks* are listed in Table 1

Table 1 Metabolites identified in *Nigella sativa* callus derived from seedling root (R) and sprout (S) via UPLC–PDA–qTOF–MS in negative ionization mode

Peak	Rt (sec)	UV (nm)	Identification	Class	Mol. ion *m/z* (−) ppm	Elemental composition	Error (ppm)	MS^n ions *m/z*	S	R
1	24.5	266	Syringic acid hexoside	Phenolic	359.11	$C_{12}H_{23}O_{12}$	4.1	145,225	–	+
2	26	ND	Methylated sucrose	Disaccharide	339.1296	$C_{13}H_{23}O_{10}$	0.2	161	+	+
3	31.5	268	1-*O*-dihdroxy phenyl acetyl glycerol	Phenolic	242.0509	$C_{11}H_{14}O_6$	3.4	163, 215	+	+
5	40.4	263	Catechin	Phenolic	289.08	$C_{15}H_{13}O_6$	2.4	243	–	+
6	44.0	265	Epicatechin	Phenolic	289.08	$C_{15}H_{13}O_6$	8.7	147, 243	+	–
7	56.6	259	Unknown	–	267.1077	$C_{10}H_{19}O_8$	3.2	147, 161	–	+
8	58.6	259, 311	*p*-Coumaroyl quinic acid	Phenolic	339.1296	$C_{13}H_{23}O_{10}$	0.1	145, 175, 207	+	–
9	82.0	263, 353	3-*O*-caffeoyl quinic acid	Phenolic	353.1449	$C_{14}H_{25}O_{10}$	1.2	179, 221, 251	+	+
10	83.2	262	Gentisic acid-*O*-glucoside	Phenolic	315.1062	$C_{14}H_{19}O_8$	7.5	175,153	–	+
11	88.0	258	Unknown	–	383.1551	$C_{15}H_{27}O_{11}$	1.4	315	+	+
12	102.8	262, 325	5-*O*-caffeoyl quinic acid	Phenolic	353.1462	$C_{14}H_{25}O_{10}$	0.6	243, 161, 179	+	+
13	147	274	Unknown	–	391.1250	$C_{16}H_{23}O_{11}$	1.5	277	+	+
14	153	269	Unknown	–	277.129	$C_{12}H_{21}O_7$	1.0	147, 175	+	–
15	160	277, 320	Nigellic acid	Monoterpene	279.233		1.1	–	+	–
16	165	302, 336	5-*O*-feruloylquinic acid	Phenolic	367.15	$C_{15}H_{27}O_{10}$	3.8	279, 211, 179	+	+
17	167	ND	Isopentyldihexoside (3-methyl-1-butanol)	Alcohol	411.1872	$C_{17}H_{31}O_{11}$	0.3	367, 237, 175	+	+
18	179	310, 336	*O*-feruloylquinic acid isomer	Phenolic	367.1610	$C_{15}H_{27}O_{10}$	0.1	235, 293	+	+
19	207	289	Benzylalcohol-*O*-pentosylhexoside	Phenolic	401.1454	$C_{18}H_{25}O_{10}$	0.2	243, 269, 293	+	+
20	218	ND	Norargemonine	Alkaloid	340.1455	$C_{20}H_{22}NO_4$	3.1	265, 175	+	+
21	227	277, 320	Nigellic acid	Monoterpene	279.1448	$C_{12}H_{23}O_7$	0.3	–	+	–
22	233	ND	Unknown	–	381.1765	$C_{16}H_{29}O_{10}$	0.4	249, 279	+	+
23	2361	358	Unknown	–	439.2173	$C_{19}H_{35}O_{11}$	2.6	249	–	+
24	242	277	Benzyl-*O*-rutinoside	Phenolic	415.1612	$C_{19}H_{27}O_{10}$	0.5	379, 317, 279	+	+
25	248	268, 290sh, 349	Kaempferol-3-*O*-hexosyl-*O*-pentoside	Flavonoid	579.2101	$C_{28}H_{35}O_{13}$	3.1	447, 285	+	+
26	272	274, 339	Quercetin-3-*O*-hexosyl-*O*-pentoside	Flavonoid	595.2044	$C_{27}H_{31}O_{15}$	2.0	301, 171	+	+
27	278	274, 339	Kaempferol-3-*O*-rutinoside	Flavonoid	595.2046	$C_{27}H_{30}O_{15}$	2.0	447, 285	+	+
28	284	ND	Hexanol pentosyl hexoside	Alcohol	395.1926	$C_{17}H_{31}O_{10}$	0.8	317, 263, 175	+	+
29	288	254, 347	Unknown	–	575.1983	$C_{25}H_{35}O_{15}$	0.3	509, 421	+	–
30	300	268, 290sh,349	Kaempferol-3-*O*-hexosyl-pentoside	Flavonoid	579.2095	$C_{28}H_{35}O_{13}$	2.1	477, 285	+	+
31	302	265	1-*O*-(dihdroxy phenyl acetyl)-glycerol	Phenolic	242.0509	$C_{11}H_{14}O_6$	3.4	325	+	+
32	333	267, 295	Quercetin	Flavonoid	300.0869	$C_{15}H_9O_7$	3	–	+	–
33	339	254, 332	Unknown	–	235.042	$C_{11}H_8NO_5$	5.5	–	+	+
34	348	ND	Unknown	–	314.1018	$C_{17}H_{16}NO_5$	4.7	235	–	+
35	358	ND	Dihydroxy octadecenoic acid	Fatty acid	313.1035	$C_{18}H_{33}O_4$	5.0	235, 277	–	+
36	355	296	Unknown	–	623.2001	$C_{29}H_{35}O_{15}$	3.2	479, 327	+	–
37	361	297	Unknown	–	235.0421	$C_{15}H_7O_3$	8.6	–	+	+
38	378	ND	Unknown	–	247.0423	$C_{16}H_7O3$	8.9	–	–	+
39	378	261	Trihydroxy octadecanoic acid	Fatty acid	329.2328	$C_{18}H_{33}O_5$	1.7	277	+	–
40	385	ND	Unknown	–	521.2623	$C_{24}H_{41}O_{12}$	3.7	419, 249	–	+

Table 1 continued

Peak	Rt (sec)	UV (nm)	Identification	Class	Mol. ion *m/z* (−) ppm	Elemental composition	Error (ppm)	MS^n ions *m/z*	S	R
41	388	257	Unknown	–	249.0579	$C_9H_{13}O_8$	8.2	_	+	–
42	400	258	Unknown	–	249.0578	$C_{16}H_9O_3$	8.8	–	+	–
43	408	ND	Unknown	–	533.1711	$C_{26}H_{29}O_{12}$	0.6	249	–	+
44	415	ND	Trihydroxy octadecadienoic acid	Fatty acid	327.2170	$C_{18}H_{31}O_5$	2.0	309, 273, 249	+	+
45	430	ND	Unknown	–	242.1756	$C_{13}H_{24}NO_3$	2.5	175	+	+
46	444	ND	Trihydroxy octadecenoic acid	Fatty acid	329.233	$C_{18}H_{33}O_5$	2.5	175, 249	+	+
47	461	ND	Unknown	–	477.2352	$C_{22}H_{37}O_{11}$	1.3	–	–	+
48	465	ND	Unknown	–	477.2352	$C_{33}H_{31}O_3$	1.0	–	–	+
49	467	256	Unknown	–	477.2262	$C_{29}H_{33}O_6$	4.3	–	–	+
50	484	263	Unknown	–	503	$C_{24}H_{39}O_{11}$	3.0	–	–	+
51	543	ND	Hederagenine-3-*O*-α-rhamnosyl dipentoside	Saponin	881.4	$C_{46}H_{73}O_{16}$	4.3	603, 471	+	–
52	549	291	Unknown	–	927.50	$C_{40}H_{79}O_{23}$	0.3	881, 689, 473	+	–
53	562	255	Unknown	–	795.4593	$C_{35}H_{71}O_{19}$	0.2	–	+	–
54	591	ND	Unknown	–	675.3618	$C_{33}H_{55}O_{13}$	3.0	317, 385, 453	+	+
55	611	ND	Unknown	–	501.3949	$C_{32}H_{53}O_4$	2.7	521, 441, 397	+	+
56	626	258	Unknown	–	383.1551	$C_{15}H_{27}O_{11}$	2.1	–	+	–
57	629	ND	Unknown	–	677.37	$C_{33}H_{5714}$	1.4	521, 339	+	+
58	636	ND	Sphingolipid IV	–	476.2779	$C_{23}H_{43}NO_7P$	3.1	453, 438	+	+
59	641	ND	Sphingolipid V	–	564.33	$C_{27}H_{51}NO_9P$	3.1	317	+	+
60	648	258	Unknown	–	559.3129	$C_{28}H_{47}O_{11}$	0.8	339, 175	+	–
61	675	255	Unknown	–	520.2788	$C_{38}H_{34}NO$	3.6	297, 175	+	–
62	676	255	Unknown	–	452.2788	$C_{28}H_{38}NO_4$	4.1	297, 175	+	+
63	681	256	Unknown	–	480.3115	$C_{30}H_{42}NO_4$	0.9		+	+
64	681	256	Unknown	–	540.3320	$C_{32}H_{46}NO_6$	1.9	295, 175	+	–
65	693	ND	Hydroxy octadecenic acid	Fatty acid	297.15	$C_{18}H_{33}O_3$	4.4	249	+	+
66	707	268	Unknown		296.1503	$C_{15}H_{22}NO_5$	4.8	–	–	+
67	764	ND	Dihydroxy octdecadienoic acid	Fatty acid	311.166	$C_{18}H_{31}O_4$	3.9	275	+	+
68	822	ND	Hydroxy tetracosanoic acid	Fatty acid	383.35	$C_{24}H_{47}O_3$	1.8	311, 271	+	+
69	873	ND	Linoleic acid	Fatty acid	279.23	$C_{18}H_{31}O_2$	3.1	–	+	–
70	916	ND	Palmitic acid	Fatty acid	255.523	$C_{16}H_{31}O_2$	2.4	–	+	+
71	931	ND	Octadecenoic acid	Fatty acid	281.24	$C_{18}H_{33}O_2$	3.8	249	+	+
72	932	ND	Oleic acid	Fatty acid	281.247	$C_{18}H_{33}O_2$	4.4	181	+	+
73	956	ND	Unknown	–	339.19	$C_{22}H_{27}O_3$	7.4	249, 155	+	+
74	1053	ND	Hydroxy docosanoic	Fatty acid	355.32	$C_{22}H_{43}O_3$	0.5	249	+	+

ND not detected, + and – denotes presence and absence of certain metabolite

Alkaloids and saponins which predominate in *N. sativa* seed extract were almost absent in callus tissue, except for minor peaks assigned as norargemonine (20) and hederagenin-*O*-α-rhamnosyldipentoside (51). Thymoquinone, the active cytotoxic agent in *N. sativa* was neither detected in callus nor its precursor glycosides. In contrast, several short chain alcohol glucosides assigned as hexanol pentosyl hexoside (28) and isopentyl dihexoside (17) were identified in callus, albeit not in seeds suggesting for an activation of short chain alcohols biosynthesis in callus; nigellic acid (15) represents another low molecular C10-monoterpene found in callus. Hydroxycinnamic acid conjugates amounted for the most abundant secondary metabolites class in callus with a total of five major peaks including *p*-coumaroylquinic acid (8), 3-*O*-caffeoylquinic acid (9), 5-*O*-caffeoylquinic acid (12) and 5-*O*-feruloyl quinic acid

(16). Another major phenypropanoid class found in both callus and seed tissue include flavonoids represented by quercetin (26 and 32) and kaempferol (25, 27, 30) flavonol glycosidic conjugates in addition to few flavans (catechin/epicatechin), though later present at much lower levels. Relative quantitative analysis revealed that fatty acids were present at much lower levels in callus compared to seeds. No significant peak differences were observed between calli derived from root and sprout tissue. This disparity in seed and callus metabolites composition is believed to be the result of induced genetic or epigenetic variation (Gould 1987) during the culturing process and/or lack of differentiation in callus cells disrupting secondary metabolism regulatory networks. *N. sativa* callus generated from seedling sprout was further exposed to MeJA phytohormone elicitor and harvested at 0, 24 and 48 h following elicitation. Elicited callus was extracted and analyzed using the same conditions to examine the nature and extent of cell differentiation on secondary metabolites biosynthesis.

Unsupervised PCA of *N. sativa* callus samples in response to MeJA elicitation

Fundamental qualitative and quantitative differences were observed between the phenolic profiles of un elicited intracellular and elicited cells as could be observed by simple visual inspection of the UPLC–MS traces of the different samples (data not shown). Nevertheless, PCA was adopted to analyze UPLC–MS spectra in a more holistic way and to identify MeJA effect on *N. sativa* metabolome. PCA is an unsupervised clustering method requiring no knowledge of the data set and acts to reduce the dimensionality of multivariate data while preserving most of the variance within (Goodacre et al. 2000). From all samples, a total of 1043 mass signals were extracted by XCMS from the UPLC–MS data set acquired in negative ionization mode. The main principal component (PC) to differentiate between samples, i.e. PC1, accounted for 79 % of the variance. Triplicate measurements from the same sample were found to be highly reproducible, as the scores of replicate measurements were more or less superimposed. The multivariate data analysis performed on MS data revealed a significant separation among samples (Fig. 2a) with the majority of samples derived from callus clearly distinguished from the *N. Sativa* samples located to the left of the vertical line representing PC1 (negative PC1 values). PCA loading plots, which define the most important components with respect to the clustering behaviour revealed that differentiation was mainly linked to hydroxycinnamates i.e., 5-*O*-caffeoyl quinic acid present at much higher levels in callus tissue, as shown from PCA loading plots (Fig. 2b). In contrast, seeds were more enriched in lipids (i.e. palmitic, oleic and linoleic fatty acids). The effect of hydroxycinnamic acid was apparent from the comparative UPLC–MS representation in Fig. 1.

Concerning callus samples elicitation, there was a strong differentiation along PC2 between callus harvested at 0 h (negative PC2 values) and cells treated with MeJA at 24 and 48 h (positive PC2 values) (Fig. 2a, right side), mainly due to a decline in 5-*O*-caffeoyl quinic acid levels concurrent with an increase in 5-*O*-feruloyl quinic acid (methylated derivative of 5-*O*-caffeoyl quinic acid) in elicited callus suggestive for an activation of distinct *O*-methyltransferase(s) (OMT) in callus tissue. Figure 3. illustrates the temporal induction profiles for 5-*O*-feruloyl quinic acid ca. five and fourfolds at 24 and 48 h post elicitation, respectively, coupled with a marked decrease in 5-*O*-caffeoyl quinic acid, presumably via an OMT enzyme up regulation targeting 5-*O*-caffeoyl quinic acid pool. Correlation analysis was performed and revealed that 5-*O*-caffeoyl quinic acid (OCQ) and 5-*O*-feruloyl quinic acid (OFQ) were negatively correlated with $r^2 = 0.76$. The relative change in OCQ and OFQ levels negates a de novo biosynthetic activation or increases in pathway precursors but is more consistent with an OCQ direct methylation reaction. Moreover, the pools of OCQ precursor, *p*-coumaroylquinic acid remained unaltered after MeJA treatment (data not shown). The increase in *O*-methyl transferase activity as a defense response to MeJA in *N. sativa* callus confirms previous molecular data showing that putrescine *N*-methyltransferases from roots of *Anisodus acutangulus* is a MeJA elicitor-responsive gene. Putrescine *N*-methyltransferase (PMT EC 2.1.1.53) catalyzes the *S*-adenosylmethionine-dependent *N*-methylation of putrescine to form *N*-methylputrescine, first committed step in tropane alkaloid biosynthesis (Kai et al. 2009). The present work provides the first metabolic evidence for an increase in an OMT activity in response to MeJA application in *N. sativa*. *O*-caffeoyl and feruloylquinic acids are important resistance factors against insect herbivores mediated via JA signaling pathway (Leiss et al. 2009). Whether feruloylquinic acid production represents another potential defense molecule in *N. sativa* against insect herbivore has yet to be fully investigated.

Activation of methylation type of reactions was also evident from the detection of methylated sucrose peak (disaccharide, peak 2) in MeJA callus, present at trace levels in control cells. Sucrose, its precursor evades detection by UPLC–MS being eluted very close to solvent front, that such decrease in its levels in response to MeJA elicitation cannot be observed. Interestingly, no significant level changes in other secondary metabolite classes i.e., flavonoids, saponins and alkaloids was detected in response to MeJA elicitation. Whether the production of methylated sucrose is an upstream event leading to the increase in OFQ level, or a parallel reaction is not clear. Sucrose is known to positively influence rosmarinic acid (an ester of caffeic acid and 3,4 dihydroxyphenyl acetic acid) accumulation in

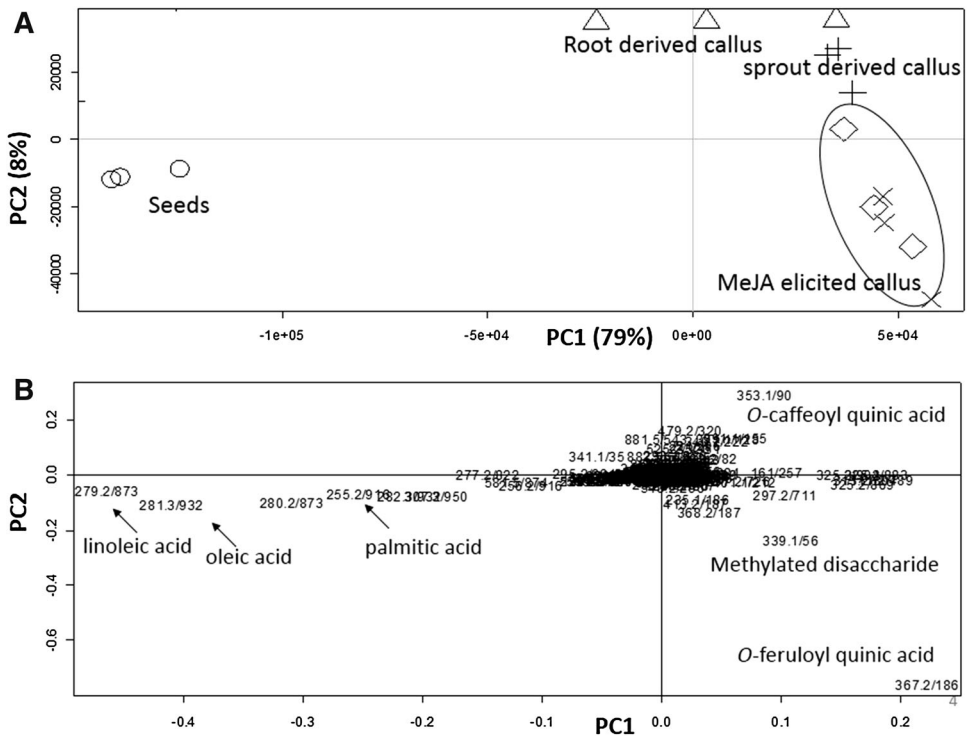

Fig. 2 UPLC–qTOF–MS (*m/z* 100–1000) principal component analyses of *Nigella sativa* seeds (*circle*), root derived callus (*triangle*), sprout derived callus (*plus*), elicited callus harvested at 24 h (*lozenge*) and 48 h (*cross*) post MeJA treatment (n = 3). The metabolome clusters are located at the distinct positions described by two vectors of principal component 1 (PC1 = 79 %) and principal component 2 (PC2 = 8 %). **a** score plot of PC1 versus PC2 scores. **b** loading plot for PC1 and PC2 with contributing mass peaks and their assignments, with each metabolite denoted by its mass/R_t (sec) pair. It should be noted that *ellipses* do not denote statistical significance, but are rather for better visibility of clusters as discussed

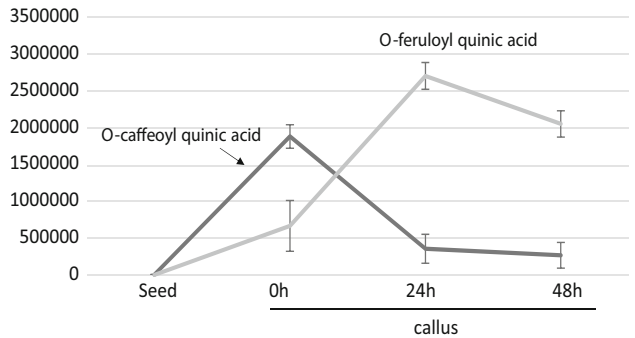

Fig. 3 Two hydroxycinnamates, *O*-caffeoylquinic acid (*black series*) and *O*-feruloylquinic acid (*grey series*) accumulation levels in *N. sativa* seeds versus unelicited and MeJA elicited callus at 24 and 48 h post elicitation. Note the increase in *O*-feruloylquinic acid levels versus a decline in its precursor *O*-caffeoylquinic acid in response to MeJA. Y axis value represents relative peak areas after normalization to the mean peak area for that compound. Results represent average of triplicate experiments ± std deviation

Ocimum sanctum cell culture (Hakkim et al. 2011). The role of methylated sucrose in plant cell has yet to be assessed; eliciting *N. sativa* callus with such a molecule could help provide stronger evidence for its role in defense repsonse.

Supervised OPLS analysis of *N. sativa* callus samples in response to Me JA elicitation

In spite of the clear separation observed in PCA analysis for callus samples harvested at 24 and 48 h post MeJA elicitation from unelicited callus and seeds, supervised OPLS-DA was further attempted to build a classification model to distinguish between seeds, elicited and unelicited calli. OPLS-DA also has greater potential in the identification of markers by providing the most relevant variables for the differentiation between two sample groups. Seed and unelicited callus were modelled against each other using OPLS-DA with the derived score plot showing a clear separation between both samples (Fig. 4b). The OPLS score plot explained 96 % of the total variance ($R^2 = 0.96$) with the prediction goodness parameter $Q^2 = 0.99$. A particularly useful tool that compares the variable magnitude against its reliability is the S-plot obtained by the OPLS-DA model and represented in Fig. 4b, where axes plotted from the predictive component are the covariance p[1] against the correlation p(cor)[1]. For the indication of plots, a cut-off value of $P < 0.05$ was used. Compared with callus, seed sample was found much more enriched in fatty acids. OPLS model (Fig. 4c) derived from modelling elicited versus unelicited callus highlights for *O*-feruloylquinic acid

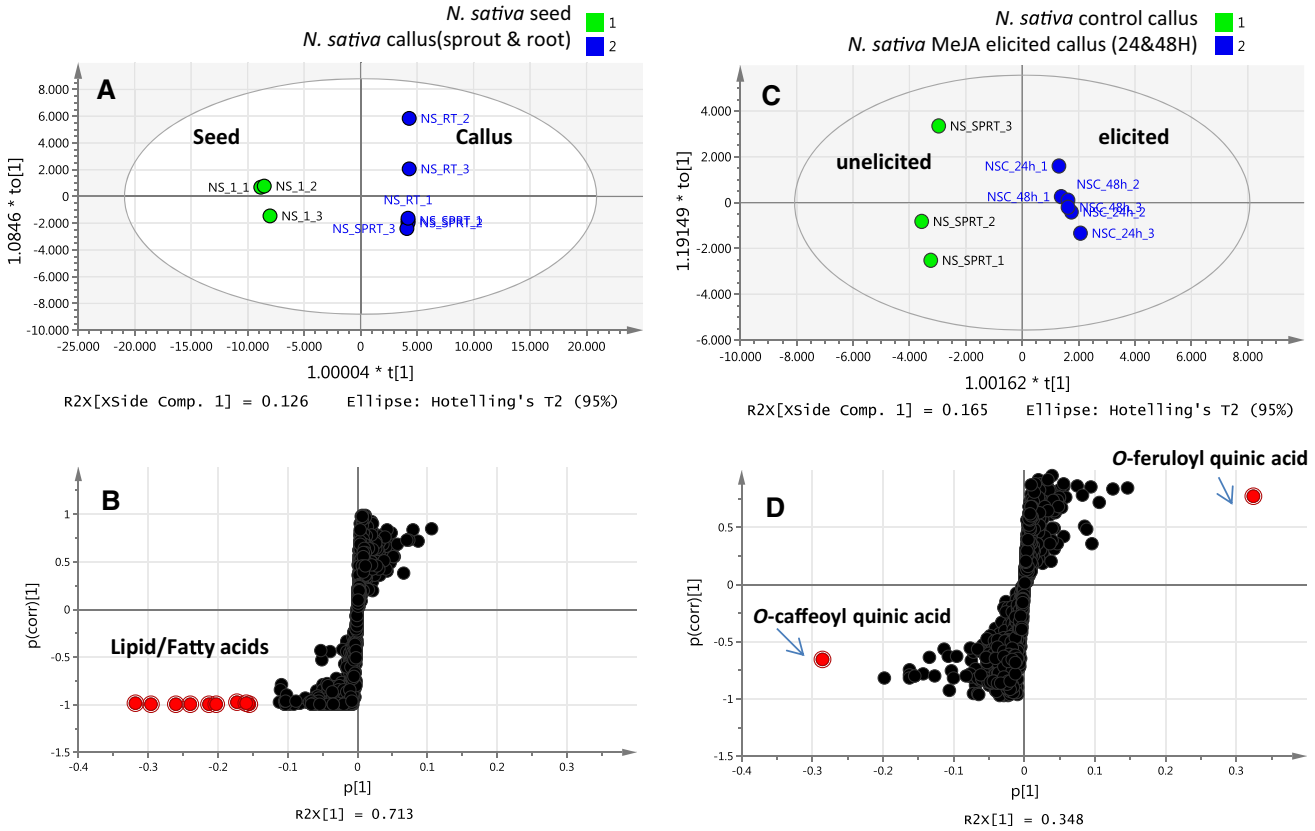

Fig. 4 UPLC–qTOF–MS (*m/z* 100–1000) orthogonal projection to latent structures-discriminant analysis (OPLS-DA) **a** OPLS-DA score plot and **b** loading S-plots derived from *N. sativa* seeds and callus samples modelled against each other. UPLC–qTOF–MS (*m/z* 100–1000) orthogonal projection to OPLS-DA **c** OPLS-DA score plot and **d** loading S-plots derived from unelicited and MeJA elicited *N. sativa* callus samples modelled against each other. The S-plot shows the covariance p[1] against the correlation p(cor)[1] of the variables of the discriminating component of the OPLS-DA model. Cut-off values of $P < 0.05$ were used; selected variables are highlighted in the S-plot with identifications are discussed in the text

peak abundance in elicited samples versus *O*-caffeylquinic acid in control callus (Fig. 4d). The attempt to build an OPLS-DA model for distinguishing root from sprout calli revealed no distinct chemical marker to distinguish between both calli (data not shown).

Conclusion

A metabolomic approach was used to investigate secondary metabolites composition and regulation in *N. sativa* callus with elicitation. To the best of our knowledge, this study provides the most comprehensive map of *N. sativa* callus polyphenols composition in comparison to seed. The results confirm and significantly extend our knowledge concerning MeJA effect on secondary metabolism in other plant species. MeJA is involved in signaling in wound responses, such as those that occur during insect herbivory (McConn et al. 1997), and *O*-caffeoylquinic acid is a well-known anti-herbivore in tobacco (Demkura et al. 2010). 5-*O*-caffeoylquinic acid is one of the lignin precursors transported from younger to older *C. canephora* leaf. Hydroxycinnamate esters play an active protective role against UV-B-induced injury (Mondolot et al. 2006). In *N. sativa* callus and as part of the MeJA elicited plant defensive response, OCQ pools appear to serve as phytoalexin precursor yielding feruloylquinic acid likely to mount a timely defense response during possible wounding or herbivory attack (see model, Fig. 5). With the provision that the present study was conducted using an artificial callus system, the marked increase in feruloylquinic acid levels in response to MeJA with a decline in its precursor suggests for a driven *OMT* enzymatic reaction. *O*-methyltransferase catalyzes the methylation of caffeic acid to ferulic acid (Shimada et al.1972; Lam et al. 2007). Probing enzymatic activity or gene expression levels involved in the biosynthesis of hydroxycinnamates could provide better understanding of its regulation in *N. sativa* callus in response to MeJA. Interestingly, transgenic *Nicotiana tabacum* lines impaired in jasmonic acid (JA) biosynthesis with

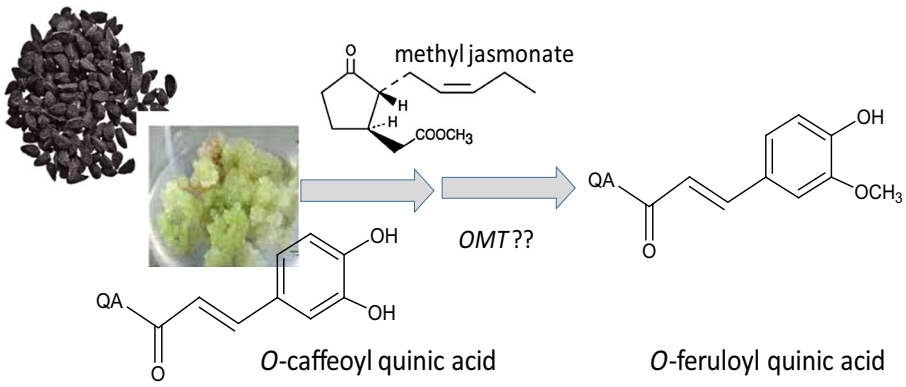

Fig. 5 Diagram showing methyl jasmonate effect on hydroxycinnamic acid pools found in *N. sativa* callus possibly mediated via induction of OMT enzyme catalyzing the methylation of *O*-caffeoylquinic acid to *O*-feruloylquinic acid. *QA* quinic acid

QA= Quinic acid

lower caffeoylquinic acid levels demonstrate reduced resistance to insect herbivore (Demkura et al. 2010). Both OCQ and OFQ were found to be induced by simulated herbivory, albeit comparative assessment of their anti-herbivore functions was not measured. Further, the identification and characterization of OMT enzyme involved in 5-*O*-feruloyl quinic acid (OFQ) production from OCQ has yet to be cloned in *N. sativa*. Both phenolics were previously identified in *N. sativa* (Farag et al. 2014) and are likely to have a defensive role. Monitoring changes in both phenolic levels in *Nigella* challenged with insect damage could provide more conclusive evidence on their role in plant insect defense. Studies focused on the molecular bases of methylation activation are ongoing and will pursue the exciting hypotheses generated using metabolomics.

References

Ahmed A, Husain A, Mujeeb M, Khan SA, Najmi AK, Siddique NA, Damanhouri ZA, Anwar F (2013) A review on therapeutic potential of *Nigella sativa*: a miracle herb. Asian Pac J Trop Biomed 3:337–352

Al-Ani NK (2008) Thymol production from callus culture of *Nigella sativa* L. Plant Tissue Cult Biotech 18:181–185

Alemi M, Sabouni F, Sanjarian F, Haghbeen K, Ansari S (2013) Anti-inflammatory effect of seeds and callus of *Nigella sativa* L. extracts on mix glial cells with regard to their thymoquinone content. AAPS Pharm Sci Tech 14:160–167

Al-Kalaf MI, Ramadan KS (2013) Antimicrobial and anticancer activity of *Nigella sativa* oil—a review Australian. J Basic Appl Sci Res 7:505–514

Al-Sheddi ES, Farshori NN, Al-Oqail MM, Musarrat J, Al-Khedhairy AA, Siddiqui MA (2014) Cytotoxicity of *Nigella sativa* seed oil and extract against human lung cancer cell line. Asian Pac J Cancer Prev 15:983–987

Banerjee S, Gupta S (1975) Morphogenesis in tissue cultures of different organs of *Nigella sativa*. Physiol Plant 33:185–187

Burits M, Bucar F (2000) Antioxidant activity of *Nigella sativa* essential oil. Phytother Res 14:323–328

Chand S, Roy SC (1979) Study of callus tissues from different parts of *Nigella sativa* (Ranunculaceae). Experientia 36:305–306

Cui L, Wang Z-Y, Zhou X-H (2013) Optimization of elicitors and precursors to enhance valtrate production in adventitious roots of *Valeriana amurensis* Smir. ex Kom. Plant Cell, Tissue Organ Cult 108:411–420

Demkura PV, Abdala G, Baldwin IT, Ballare CL (2010) Jasmonate-dependent and-independent pathways mediate specific effects of solar ultraviolet B radiation on leaf phenolics and antiherbivore defense. Plant Physiol 152:1084–1095

Farag MA, Wessjohann LA (2012) Metabolome classification of commercial *Hypericum perforatum* (St. John's Wort) preparations via UPLC-qTOF-MS and chemometrics. Planta Med 78:488–496

Farag MA, Deavours BE, de Fátima A, Naoumkina M, Dixon RA, Sumner LW (2009) Integrated metabolite and transcript profiling identify a biosynthetic mechanism for hispidol in *Medicago truncatula* cell cultures. Plant Physiol 151:1096–1113

Farag MA, EL-Ahmady S, Alian F, Wessjohann LA (2013) Metabolomics driven analysis of artichoke leaf and its commercial products via UHPLC-q-TOF-MS. Phytochemistry 95:177–187

Farag MA, Gad HA, Heiss AG, Wessjohann LA (2014) Metabolomics driven analysis of six *Nigella* species seeds via UPLC-qTOF-MS and GC-MS coupled to chemometrics. Food Chem 151:333–342

Goodacre R, Shann B, Gilbert RJ, Timmins EM, McGovern AC, Alsberg BK, Kell DB, Logan NA (2000) Detection of the dipicolinic acid biomarker in Bacillus spores using Curie-point pyrolysis mass spectrometry and Fourier transform infrared spectroscopy. Anal Chem 72:119–127

Gould AR (1987) Staining and nuclear cytology of cultured cells. In: Vasil IK (ed) Cell culture and somatic cell genetics of plants, vol 1. Academic Press, New York, pp 698–710

Grata E, Boccard J, Guillarme D, Glauser G, Carrupt PA, Farmer EE, Wolfender JL, Rudaz S (2008) UPLC–TOF-MS for plant metabolomics: a sequential approach for wound marker analysis in *Arabidopsis thaliana*. J Chromatogr B 871:261–270

Guo ZJ, Lamb C, Dixon RA (1998) Potentiation of the oxidative burst and isoflavonoid phytoalexin accumulation by serine protease inhibitors. Plant Physiol 118:1487–1494

Hakkim FL, Kalyanib S, Essaa M, Girija S, Song H (2011) Production of rosmarinic in *Ocimum sanctum* cell cultures by the influence of sucrose, phenylalanine, yeast extract, and methyl jasmonate. Int J Biol Med Res 2:1070–1074

Houghton PJ, Zarka R, de las Heras B, Hoult JR (1995) Fixed oil of *Nigella sativa* and derived thymoquinone inhibit eicosanoid generation in leukocytes and membrane lipid peroxidation. Planta Med 61:33–36

Kai G, Zhang Y, Chen J, Li L, Yan X, Zhang R, Liao P, Lu X, Wang W, Zhou G (2009) Molecular characterization and expression analysis of two distinct putrescine N-methyltransferases from roots of *Anisodus acutangulus*. Physiol Plant 135:121–129

Khan MA (1999) Chemical composition and medicinal properties of *Nigella sativa* Linn. Inflammopharmacology 7:15–35

Kumara SS, Huat BT (2001) Extraction, isolation and characterization of anti-tumour principle, α-hedrin, from the seeds of *Nigella sativa*. Planta Med 67:29–32

Lam KC, Ibrahim RK, Behadad B, Dayanandans S (2007) Structure, function and evolution of plant *O*-methyltransferase. Genome 50:1001–1013

Leiss KA, Maltese F, Choi YH, Verpoorte R, Klinhamer PGL (2009) Identification of chlorogenic acid as a resistance factor for thrips in chrysanthemum. Plant Physiol 150:1567–1575

Liu X, Abd El-Aty AM, Shim JH (2011) Various extraction and analytical techniques for isolation and identification of secondary metabolites from *Nigella sativa* seeds. Mini Rev Med Chem 11:947–955

Mabry T, Markham K, Thomas M (1970) The systematic identification of flavonoids. Springer, Berlin, Heidelberg, New York, pp 230–270

McConn M, Creelman RA, Bell E, Mullet JE, Browse J (1997) Jasmonate is essential for insect defense in Arabidopsis. Proc Natl Acad Sci USA 94:5473–5477

Moghaddasi SM (2011) *Nigella sativa* traditional usages (Black seed). Adv Environ Biol 5:5–16

Mondolot L, Fisca P, Buatois B, Talansier E, De Kochko A, Campa C (2006) Evolution in caffeoylquinic acid content and histolocalization during *Coffea canephora* leaf development. Ann Bot 98:33–40

Rafati S, Niakan M, Naseri M (2014) Anti-microbial effect of *Nigella sativa* seed extract against staphylococcal skin infection. Med J Islam Repub Iran 28:42

Randhawa MA, Alghamdi MS (2011) Anticancer activity of *Nigella sativa* (black seed), a review. Am J Chin Med 39:1075–1091

Salem ML, Hossain MS (2000) Protective effect of black seed oil from *Nigella sativa* against murine cytomegalovirus infection. Int J Immun Pharmacol 22:729–740

Shimada M, Fushiki H, Higuchi T (1972) *O*-methyltransferase activity from Japanese black pine. Phytochemistry 11:2657–2662

Smith CA, Want EJ, O'Maille G, Abagyan R, Siuzdak G (2006) XCMS: processing mass spectrometry data for metabolite profiling using nonlinear peak alignment matching, and identification. Anal Chem 78:779–787

Sultan MT, Butt MS, Karim R, Iqbal SZ, Ahmad S, Zia-Ul-Haq M, Aliberti L, Ahmad NA, Feo VD (2014) Effect of *Nigella sativa* fixed and essential oils on antioxidant status, hepatic enzymes, and immunity in streptozotocin induced diabetes mellitus. BMC Compl Altern Med 14:193

Sumner LW, Lei Z, Nikolau BJ, Saito K (2014) Modern plant metabolomics: advanced natural product gene discoveries, improved technologies, and future prospects. Nat Prod Rep 32:212–229

Timperio AM, d'Alessandro A, Fagioni M, Magro P, Zolla L (2012) Production of the phytoalexins trans-resveratrol and delta-viniferin in two economy-relevant grape cultivars upon infection with *Botrytis cinerea* in field conditions. Plant Physiol Biochem 50:65–71

Xuan NT, Shumilina E, Qadri SM, Götz F, Lang F (2010) Effect of thymoquinone on mouse dendriticcells. Cell Physiol Biochem 25:307–314